UDC 621.3 https://doi.org/10.20998/2074-272X.2024.2.04

A. Chaib Ras, R. Bouzerara, H. Bouzeria

An adaptive controller for power quality control in high speed railway with electric locomotives with asynchronous traction motors

Introduction. *Power quality in an electric railway system pertains to the dependability, consistency, and purity of the electrical power provided to different components and systems within the railway infrastructure. Assessing power quality offers considerable opportunities to improve the efficiency of railway systems.* ***Problem.*** *Managing the flow of active and reactive power effectively, decreasing harmonic currents, and addressing the negative sequence component are all critical parts of improving power quality for electrified rail systems. As a result, flexible AC transmission systems are the major means of minimizing or decreasing these difficulties.* ***Purpose.*** *This study describes a half-bridge reactive power railway power conditioner (HB-RPC) with a novel Ynev balancing transformer. HB-RPC is made up of four switching devices and two DC capacitors and the compensator's stability is determined by the operating voltage of the DC-link. Any variations or imbalances in the DC voltage might cause the compensator to operate in an unstable manner.* ***Novelty.*** *Of a novel balanced transformer with HB-RPC in a high-speed railway system with two scenarios.* ***Methods.*** *The study utilized MATLAB/Simulink software for simulation purposes. The system integrates a fuzzy logic controller (FLC) and a PI controller to optimize DC voltage, ensuring its constancy and balance, with the objective of improving the overall stability of the system.* ***Results.*** *The simulation outcomes illustrate the efficacy of the control approach. Through a comparison of results between scenarios (two and four trains) with the PI-based-HB-RPC and the FLC-based-HB-RPC, the system exhibits enhanced stability for the proposed railway system when employing the FLC-based-HB-RPC, compared to a controller based on PI.* ***Practical value.*** *The proposed configuration elucidates its role in enhancing both the dynamic performance of the system and the power quality of the three-phase rail traction chain.* References 21, table 6, figures 21.
Key words: **railway power conditioner, Ynev transformer, fuzzy logic controller, PI controller, asynchronous motor, power quality, electric railway system.**

Вступ. *Якість електроенергії в системі електричних залізниць відноситься до надійності, сталості та чистоти електроенергії, що подається різним компонентам та системам залізничної інфраструктури. Оцінка якості електроенергії відкриває значні можливості підвищення ефективності залізничних систем.* ***Проблема***. *Ефективне керування потоками активної та реактивної потужності, зниження гармонійних струмів та усунення компонента зворотної послідовності – все це важливі частини покращення якості електроенергії для електрифікованих залізничних систем. В результаті гнучкі системи передачі змінного струму є основним засобом мінімізації чи зменшення цих труднощів.* ***Мета***. *У цьому дослідженні описується напівмостовий стабілізатор реактивної потужності залізниці (HB-RPC) з новим балансуючим трансформатором Ynev. HB-RPC складається з чотирьох перемикаючих пристроїв та двох конденсаторів постійного струму, а стабільність компенсатора визначається робочою напругою ланки постійного струму. Будь-які зміни або дисбаланс напруги постійного струму можуть призвести до нестабільної роботи компенсатора.* ***Новизна***. *Стосується нового балансного трансформатора з HB-RPC у системі високошвидкісних залізниць із двома сценаріями.* ***Методи***. *У дослідженні використовувалося програмне забезпечення MATLAB/Simulink з метою моделювання. Система поєднує контролер нечіткої логіки (FLC) та ПІ-регулятор для оптимізації напруги постійного струму, забезпечення його сталості та балансу з метою покращення загальної стабільності системи.* ***Результати***. *Результати моделювання ілюструють ефективність підходу до управління. За допомогою порівняння результатів сценаріїв (два та чотири поїзди) з HB-RPC на основі ПІ та HB-RPC на основі FLC система демонструє підвищену стабільність для запропонованої залізничної системи при використанні HB на основі FLC-RPC, у порівнянні з контролером з застосуванням ПІ.* ***Практична цінність***. *Запропонована конфігурація пояснює її роль у підвищенні як динамічних характеристик системи, так і якості електроенергії трифазного залізничного тягового кола.* Бібл. 21, табл. 6, рис. 21.
Ключові слова: **залізничний стабілізатор напруги, Ynev трансформатор, контролер нечіткої логіки, ПІ-регулятор, асинхронний двигун, якість електроенергії, електрична залізнична система.**

Introduction. The configuration and utilization of electrified railways are well-established [1]. With the surge in rail traffic and widespread adoption of modern traction vehicles equipped with sinusoidal current absorption rectifiers, electric transport systems have become substantial single-phase loads for the traction supply system. Additionally, they function as nonlinear loads, consuming reactive power and giving rise to power factor and stability issues. Consequently, electric trains contribute to imperfections in the railway supply, including negative sequence current (NSC), reactive power and harmonics [1].

Enhancing energy efficiency and ensuring high-quality performance have become imperative across various technical domains today. The prevalent power quality issues typically fall into two main categories: voltage irregularities and harmonic distortion [2]. The traction power system can be segmented into four components, namely the upstream power system (three-phase power system), the traction power substation, the overhead contact line system, and the electric train, as illustrated in Fig. 1 [1].

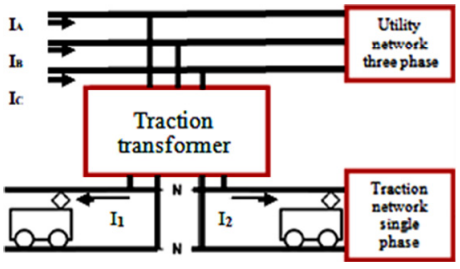

Fig. 1. Synoptic of traction chain system

The high-voltage network faces challenges due to the uncertainty, non-linearity, and asymmetry introduced by traction loads, resulting in the presence of NSC and harmonics. The asymmetry and non-linearity within the traction power supply system contribute to more significant issues for the power grid, including imbalances and harmonic disturbances. The characteristics of locomotives,

utilizing power electronics techniques to adjust speed, make them non-linear loads. In this scenario, these loads act as sources of harmonics while also operating as single-phase loads. This is the reason why the traction system can extract two single-phase electric powers from a three-phase power supply [3, 4], introducing a lot of power quality challenges to the three-phase power system, ultimately impacting the operation of electrical equipment and the network.

Various methods have been used to improve the power quality of three-phase power systems in order to maintain the dependability and balance of electrical railway power systems. This entails reducing the impacts of nonlinear traction loads on three-phase power systems [5] through the use of Flexible AC Transmission Systems (FACTS) [6]. In particular, the use of balance transformers (such as Scott, YNvd, Leblanc, and others) has been a prominent technique to addressing this difficulty [7, 8]. Balancing transformers possess the capability to transform a three-phase system into a two-phase system, thereby reducing NSC on the secondary side under equal load conditions [9].

However, it is important to note that employing balancing transformers alone is insufficient to enhance power quality in the railway traction system. Consequently, the integration of a compensator into the traction system has become essential.

Enhancing the efficiency and rapid control features of these technologies has spurred research into various FACTS devices [10-12]. The selection of specific FACTS devices depends on the intended purpose, leading to their connection in configurations such as shunt, series, series-series and series-shunt [13, 14]. The compensator's overall performance is fundamentally shaped by the configuration of the controller being manipulated.

The aim of this study is to implement a control method for the suggested half-bridge reactive power railway power conditioner (HB-RPC) with Ynev. Consequently, a fuzzy logic controller (FLC) with 49 rules based on HB-RPC is developed to govern the outputs of two power switching legs, thereby enhancing the overall performance of the power system. Subsequently, the achieved outcomes are contrasted with those obtained using a PI controller. This comparison aims to elucidate which controller exerts a more significant influence on the dynamic stability of the traction system under different loads. The paper provides a detailed description of the traction power substation, the transformer connections, and the structure of the HB-RPC.

The system operation and the control method for the compensator under Ynev are described. Trains (asynchronous motors) are used as loads to validate the performance of the system. The most important power quality issues in electrified railways have been investigated here. Results and discussion are analyzed and concluded in this study.

Modeling of proposed system. For studying the performance of our system, an electrified railway system as illustrated in Fig. 2 is proposed.

The Ynev transformer principles. The traction loads operate as single-phase loads within a three-phase system. Consequently, balanced transformers are employed in the power supply system to generate two-phase output from the three-phase system, effectively addressing power quality issues such as the elimination of zero sequence current and reduction of NSC. In [7, 8], various connection configurations are illustrated, each transformer possessing distinct advantages and disadvantages. The selection of a specific configuration is contingent on three key factors: Transformer Utilization Factor (TUF), Line Utilization Factor (LUF), and the current unbalance ratio ε.

$$TUF \equiv SR/ST\,; \tag{1}$$

$$LUF \equiv SR/SL\,; \tag{2}$$

$$\varepsilon \equiv \left|I^-\right| \Big/ \left|I^+\right|, \tag{3}$$

where SR, ST, SL are the maximum utilization capacities for the system, transformer and line, respectively; I^-, I^+ are the negative and positive sequence currents.

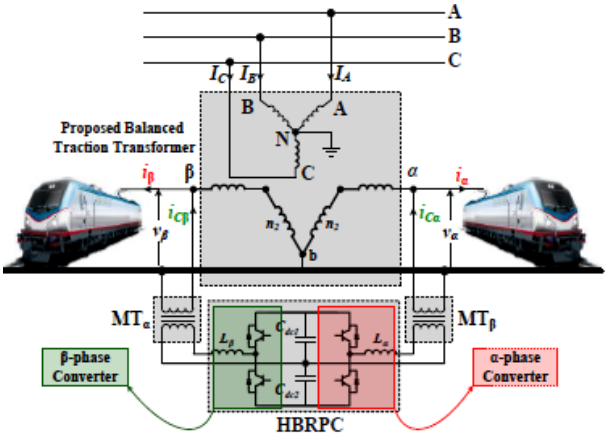

Fig. 2. The proposed electrified railway system

This study involves the transformation of a three-phase system into a single-phase system using a Ynev two-phase balanced transformer (Fig. 3), wherein the primary three-phase winding is interconnected in a star configuration with a grounded neutral point.

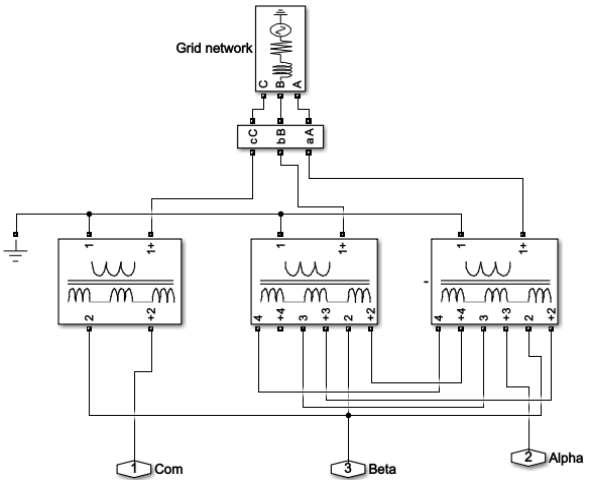

Fig. 3. Ynev transformer wiring diagram

This transformation not only enhances system protection but also involves a secondary winding connected in an open delta configuration [9-15]. The magnitudes of the mathematical voltage expressions on the secondary side are:

$$\left|v_\alpha\right| = \sqrt{3}V\left(N_2^2 + N_3^2 + N_2N_3\right)^{1/3}; \tag{4}$$

$$\left|v_\beta\right| = \sqrt{3}V\left(N_2^2 + N_3^2 + N_2N_3\right)^{1/3}, \tag{5}$$

where N_2, N_3 are the turn ratios associated with the windings of the transformer.

The current relationships can be expressed as:

$$\begin{bmatrix} I_A \\ I_B \\ I_C \end{bmatrix} \equiv \begin{bmatrix} (N_2+N_3) & -N_3 \\ -N_3 & (N_2+N_3) \\ -N_2 & -N_2 \end{bmatrix} \begin{bmatrix} I_\alpha \\ I_\beta \end{bmatrix}, \quad (6)$$

where I_A, I_B, I_C are the primary side's phase currents; I_α, I_β are the secondary side's two-phase currents.

The components of three-phase currents zero sequence I^0, positive sequence I^+, and negative sequence I^- currents are:

$$\begin{bmatrix} I^0 \\ I^+ \\ I^- \end{bmatrix} \equiv \frac{1}{3} \begin{bmatrix} 0 & 0 \\ N_2(1-\alpha^2)+N_3(1-\alpha) & N_2(\alpha-\alpha^2)+N_3(\alpha-1) \\ N_2(1-\alpha)+N_3(1-\alpha^2) & N_2(\alpha^2-\alpha)+N_3(\alpha^2-1) \end{bmatrix}. \quad (7)$$

Load model. In this paper, we model an electric locomotive train, illustrated in Fig. 4, each asynchronous motor driven by two inverters controlled through pulse width modulation. The system incorporates static power converters to transform the physical characteristics, specifically voltage, prior to reaching the traction motor.

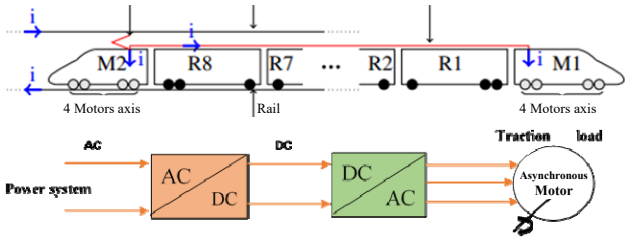

Fig. 4. High speed train's traction circuit schematic diagram

HB-RPC configuration. HB-RPC is one of the FACTS devices that have been specifically designed for railway traction power supply [11]. As illustrated in Fig. 5, HB-RPC is made up of four switching devices and two DC capacitors, which reduces the number of switches compared to a normal railway power conditioner (RPC). As a result, this structure is employed to lower the cost and complexity of the control. It is utilized to manage active and reactive power flow, as well as harmonics suppression.

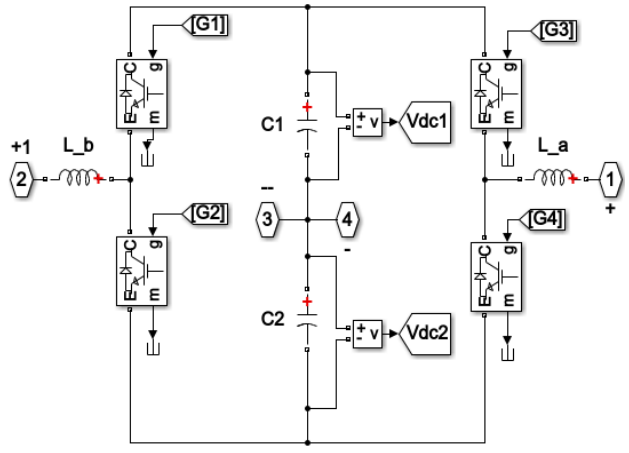

Fig. 5. HB-RPC topology proposed in MATLAB

The Ynev transformer's secondary side is linked to the half-bridge converters through a pair of step-down transformers and inductors. This setup is designed to mitigate the transmission of harmonics and reactive power through the transformer. In this arrangement, each side of the traction power substation accommodates two electric trains (in the 1st case) and four trains (in the 2nd case), with i_α and i_β representing the currents of sections α and β, and denoting the compensating currents.

To address symmetrical and sinusoidal waveforms in the secondary side currents (i_α, i_β), the HB-RPC introduces compensatory currents ($i_{C\alpha}$, $i_{C\beta}$) into the system through interface inductances (L_α, L_β) and step-down transformers.

The load currents can be written as [9-16]:

$$\begin{cases} I_{L\alpha}(t) \equiv \sqrt{2} L_{LP\alpha} \cos(\omega t + \theta_1) + \sum_{h=2} \sqrt{2} I_{h\alpha} \cos(\omega t + \theta_{h\alpha}); \\ I_{L\beta}(t) \equiv -\sqrt{2} I_{LP\beta} \cos(\omega t + \theta_2) + \sum_{h=2} \sqrt{2} I_{h\beta} \cos(\omega t + \theta_{h\beta}), \end{cases} \quad (8)$$

where $I_{h\alpha}$, $I_{h\beta}$ are the h^{th} order harmonic currents of the α and β phases, respectively; $\theta_{h\alpha}$, $\theta_{h\beta}$ are the phases degree of h^{th} order harmonic currents of the α and β phases; θ_1, θ_2 are the phase difference between α and β phases; $I_{LP\alpha}$, $I_{LP\beta}$ are the active components.

The compensation currents ($I_{C\alpha}$, $I_{C\beta}$) for the two half-bridge converters can be expressed as:

$$\begin{cases} I_{C\alpha} = I_\alpha(t) - I_{ref\alpha}(t); \\ I_{C\beta} = I_\beta(t) - I_{ref\beta}(t), \end{cases} \quad (9)$$

where I_α, I_β are the secondary side currents; $I_{ref\alpha}$, $I_{ref\beta}$ are the reference currents.

The connection between the compensation currents and the reference currents can be established as:

$$\begin{cases} I_{ref\alpha}(t) = \sqrt{\frac{2}{3}} I_{mp} \cos \omega t; \\ I_{ref\beta}(t) = \sqrt{\frac{2}{3}} I_{mp} \left(\cos \omega t - \frac{2\pi}{3} \right), \end{cases} \quad (10)$$

where I_{mp} is the DC component:

$$I_{mp} = \frac{1}{2} I_{LP\alpha} + I_{LP\beta}, \quad (11)$$

where $I_{LP\alpha}$, $I_{LP\beta}$ are the active components of two loads currents of traction power arms.

Operation and control method of the system.

A. Operation of the HB-RPC involves the dynamic exchange of power between sides, achieving the transfer and equilibrium of active power, and compensating reactive power to meet the load requirements. This is accomplished by charging or discharging capacitors $C1$, $C2$ as illustrated in Fig. 6, 7, representing the primary goal of the HB-RPC [16-18]. The operations modes of HB-RPC are next:

- when the supply current $i > 0$: the charging mode of the DC-link capacitor, diode $D1$ is conducted and the discharging mode of the DC-link capacitor, power switch $S2$ is conducted (Fig. 6);
- when the supply current $i < 0$: $S1$ is conducted, the capacitor $C1$ is discharging, and $|i|$ starts to increase, when $D2$ is conducted, the capacitor $C2$ is charging, and $|i|$ starts to decrease (Fig. 7).

B. DC-link voltage control. The utilization of two capacitors gives rise to a voltage balance issue. To address this and attain dynamic energy equilibrium, two FLC and PI controllers are suggested. These controllers generate the reference current signals for phases A, B, C along with a compensator to maintain the DC-link voltage stability and minimize power losses.

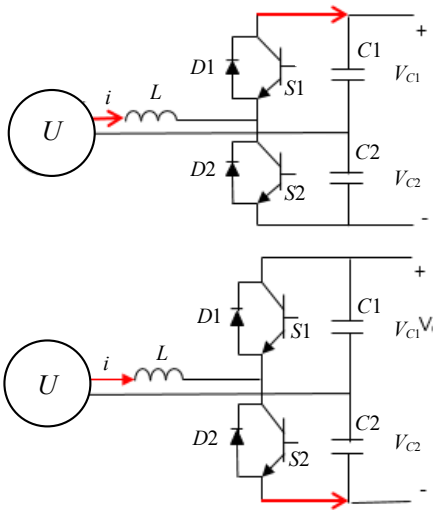

Fig. 6. Charging (above) and discharging (below) mode of HB-RPC for the supply current $i > 0$

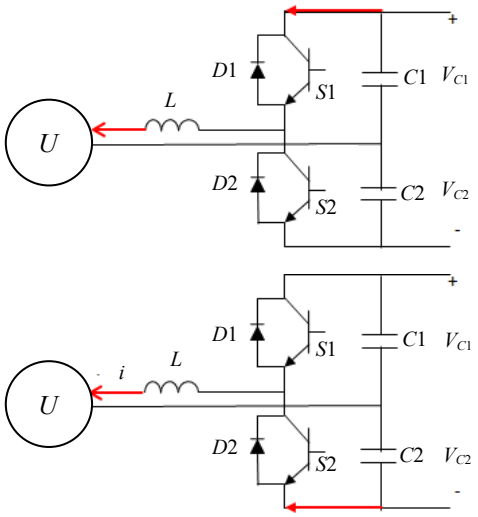

Fig. 7. Charging (above) and discharging (below) mode of HB-RPC for the supply current $i < 0$

Approach utilizing a FLC. It is a mathematical framework designed to assess analog input values in the context of logical variables with continuous values ranging from 0 to 1 [14-19]. FLCs are particularly well-suited for addressing uncertain control problems. The FLC is structured into 3 components: fuzzification, fuzzy inference, and defuzzification (Fig. 8) [20, 21].

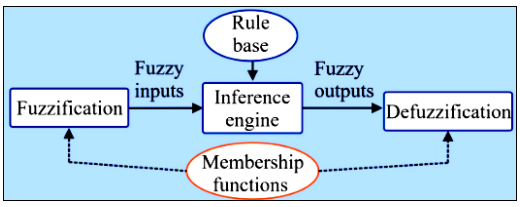

Fig. 8. Architecture of FLC

Fuzzification is the process of transforming crisp inputs values into language values represented by membership functions. FLC's inputs are designated as the error (e) in DC-link voltage and derivate error (de) at simple times t [15]:

$$\begin{cases} e(t) = V_{dc_{ref}}(t) - V_{dc}(t); \\ \mathrm{d}e(t) = e(t) - e(t-1). \end{cases} \quad (12)$$

Common types of input membership functions include triangular, trapezoidal, or exponential shapes.

In our study, we used triangle membership (Fig. 9). Seven linguistic variables for both inputs and output were selected as results there are 49 rules for FLC.

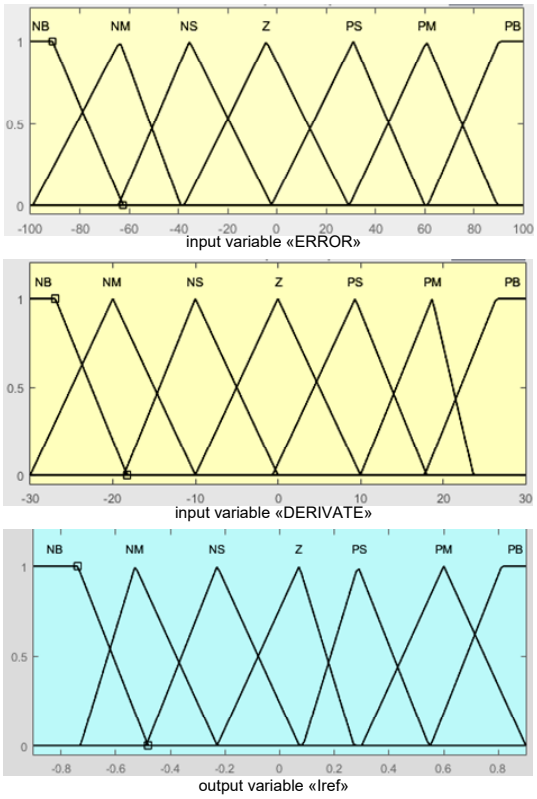

Fig. 9. Membership functions of fuzzy system

The inference engine plays a crucial role in fuzzy logic operations by linking membership functions with fuzzy rules to produce a fuzzy output. Memdani method is employed to execute this process. On the other hand, defuzzification is the opposite of fuzzification, involving the conversion of fuzzy quantities into precise values. In our case, the center of gravity is employed to calculate the output of the FLC, specifically the reference current as outlined in Table 1.

Table 1

Rule base of FLC

de/e	NB	NM	NS	Z	PS	NM	PB
NB	NB	NB	NB	NM	NM	NS	Z
NM	NB	NB	NM	NM	NS	Z	PS
NS	NB	NM	NM	NS	Z	PS	PM
Z	NM	NM	NS	Z	PS	PM	PM
PS	NM	NS	Z	PS	PM	PM	PB
PM	NS	Z	PS	PM	PM	PB	PB
PB	Z	PS	PM	PM	PB	PB	PB

Figure 9 illustrates the membership functions of the input and output variables in the fuzzy system, while Fig. 10 displays the surface of fuzzy rules.

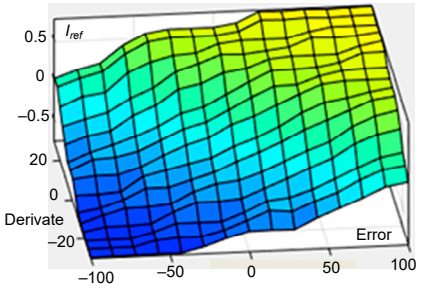

Fig. 10. Fuzzy rules surface

The configuration block of the compensator control system for HB-PRC is shown in Fig. 11.

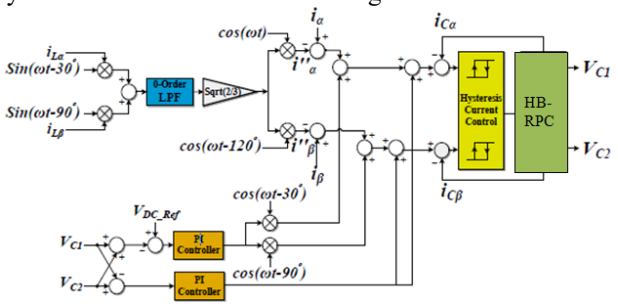

Fig. 11. HB-RPC control system with FLC

PI controller approach. The PI controller's efficiency in limiting steady-state error, as well as its ease of implementation, are the grounds for its extensive application. Figure 12 shows the PI controller principle and the configuration block of the compensator control system for HB-PRC.

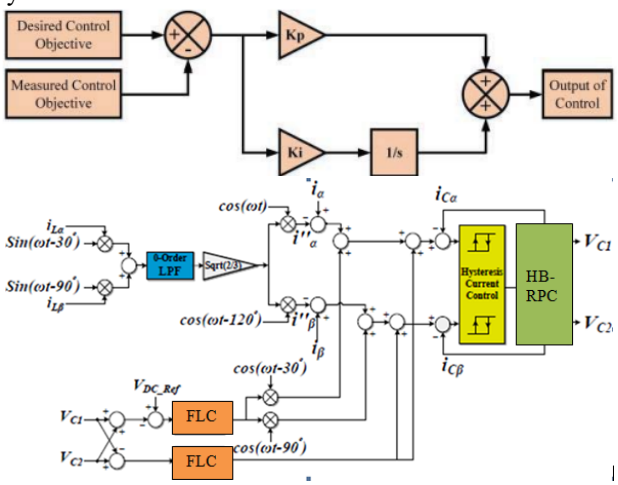

Fig. 12. HB-RPC control system with PI

Results and discussion. The aforementioned test system was created in MATLAB/Simulink. This section is further divided into two scenarios:

- case (1) has HB-RPC in high-speed railway system with 2 trains;
- case (2) has the HB-RPC with 4 trains.

A comparison of the DC-link voltages and simulation results for scenario (1) and (2) is performed, taking into account both scenarios with and without a compensator and controller. The simulations were utilized to verify the effectiveness of the proposed compensator and control method, as well as to evaluate the new transformer's ability to alleviate NSC.

A standard electrical traction system was selected to facilitate an authentic comparative case study between FLC and PI controllers with two scenarios with varying load conditions are examined to analyze the influence of the proposed topology. The assumed values for the public electrical grid voltage are 230 kV, and its secondary side provides a 27.5 kV supply to the traction loads. In the analysis of our electric railway system, electric locomotives are modeled as asynchronous motors, which representing nonlinear loads and providing a suitable basis for result evaluation.

The compensator is linked in parallel with the three-phase power system. The specific parameters of the chosen traction system are outlined in Table 2.

Table 2
Simulation parameters

Transformer (class TPS) ratio	230 kV / 27.5 kV
Ynev transformer ratio	27.5 / 1
Interface inductance, mH	4
DC-link capacitors, mF	40
Nominal power, MW	10
Voltage of DC capacitor Vdc_{ref}, V	2000

The controller is used to correct the error between the reference value of the DC-link voltage Vdc_{ref} and the instantaneous actual value V_{dc}. The HB-RPC's controller should issue instructions for the compensation currents to be injected, followed by the acquisition of sinusoidal and symmetrical currents on the three-phase electrical grid side without the NSC and to transfer active and reactive energy from one segment to another.

The DC-link voltage is displayed in Fig. 13, at t = 0.5 s, the HB-RPC is activated the V_{dc} voltage following to the reference signal Vdc_{ref}. It is clearly observed that the DC-link voltage stable and regulated (reducing the voltage fluctuation) better with the FLC compared to the PI. Fuzzy control demonstrates robustness by efficiently managing variables with distinct fuzzy logic and facilitating the enhancement of fuzzy rules. The utilization of fuzzy control for refining compensation contributes to improved performance in achieving better compensation outcomes.

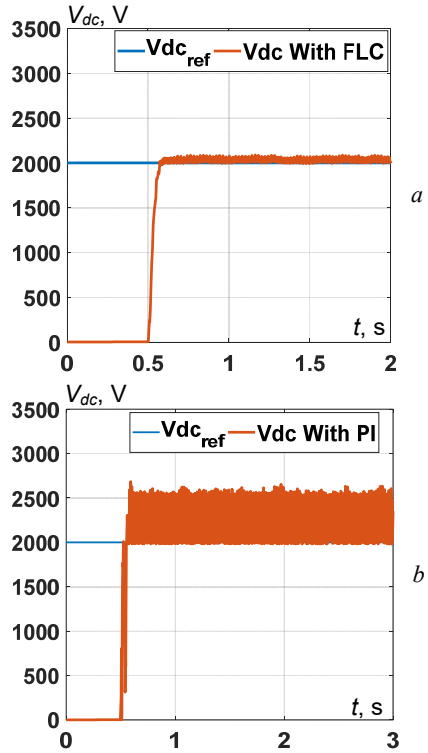

Fig. 13. DC-link voltage with FLC (*a*) and with PI (*b*)

Case I with two trains. The currents of the primary side and the secondary side are shown in Fig. 14; I_A, I_B and I_C are unbalanced and unequal, when the compensator turned off, which contain NSC but after the HB-RPC is turned on at 0.5 s, the currents are more stable (balanced, equal, phase difference 120°). It is clear appeared that the time response of the compensator with the FLC is less than the PI.

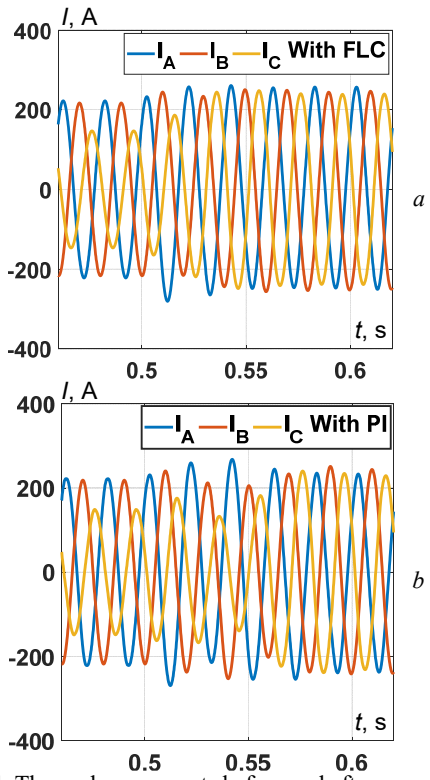

Fig. 14. Three-phase currents before and after compensation with FLC (*a*) and with PI (*b*) for Case I

In Fig. 15, as we can see the secondary current of the transformer I_α, I_β are balanced even before turned on the HB-RPC, which confirms the transformer's ability to reduce the imbalance.

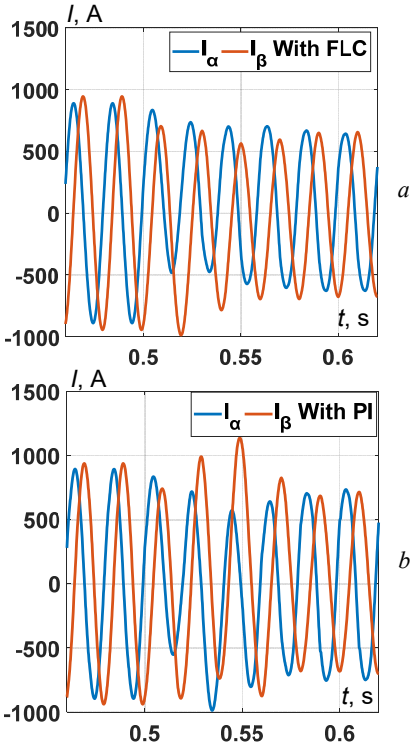

Fig. 15. The secondary side current of the traction transformer with FLC (*a*) and with PI (*b*) for Case I

Figure 16 presents the compensation current $I_{C\alpha}$, $I_{C\beta}$. After 0.5 s the present current is sinusoidal which shows that it includes most effective active current without harmonics, which can induced balanced three-phase currents on the power grid.

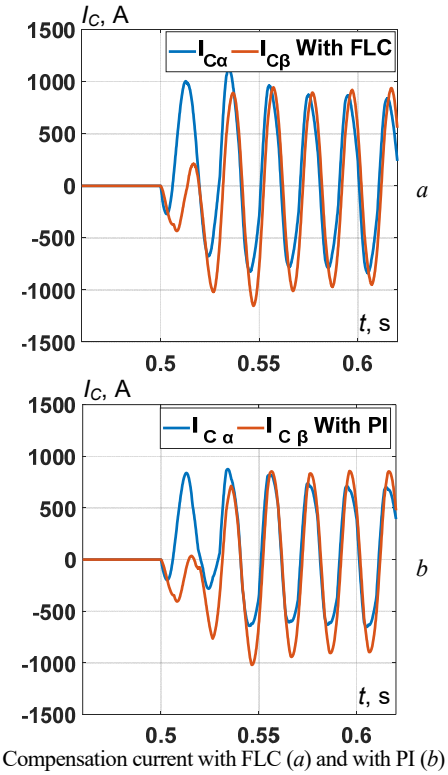

Fig. 16. Compensation current with FLC (*a*) and with PI (*b*) for Case I

According to Fig. 17, which shows the NSC which is reduced to almost zero and explain the symmetrical three-phase current. We called the relationship between the NSC and PSC the current unbalance ration. Table 3 represents the ratio index before and after the HB-RPC start working.

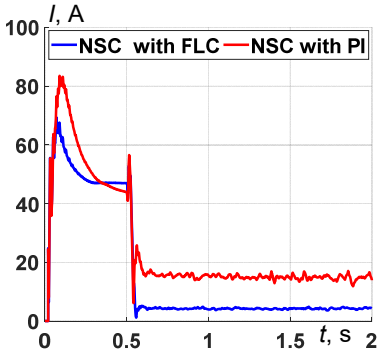

Fig. 17. Negative sequence currents with FLC and PI for Case I

Table 3

NSC ratio in the public electrical grid current with PI and FLC

HB-RPC integrate	Before	After
Time, s	0 – 0.4	0.5 – 2
PI, %	25	2.08
FLC, %		1.17

Table 4 shows the FFT analysis results before and after the compensation of the currents at the phases *A*, *B* and *C*; it is observed that the performance of the HB-PRC and Ynev transformer with the FLC is superior to the PI controller for harmonic elimination.

Table 4

THD compensation results

Cases 2 trains	I_A	I_B	I_C
Without compensation, %	7.88	8.94	13.68
Compensation / FLC, %	1.18	0.92	1.51
Compensation / PI, %	3.16	1.69	2.74

Case II with four trains. The loading situation, which was created by delivering a step load to the system, was simulated in order to stress the system with a high-power variation for a stability test.

Figures 18, 19 illustrate the simulation outcomes corresponding to case II. In this scenario, the absence of a compensator (no HB-RPC) interval is associated with elevated levels of nonlinear signal components and harmonics, necessitating compensation.

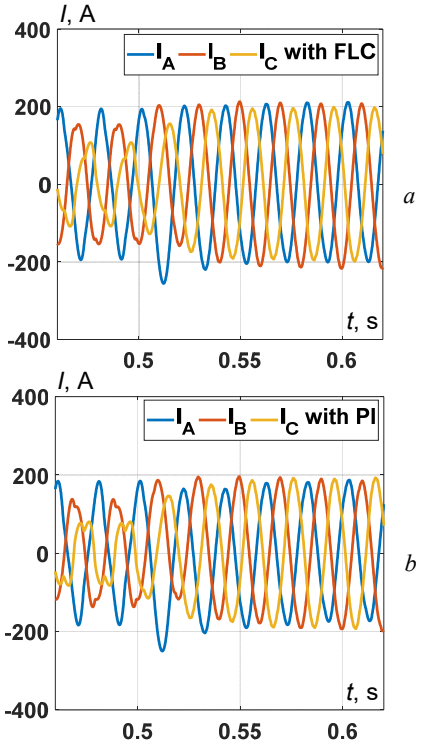

Fig. 18. Three-phase currents before and after compensation with FLC (*a*) and with PI (*b*) for Case II

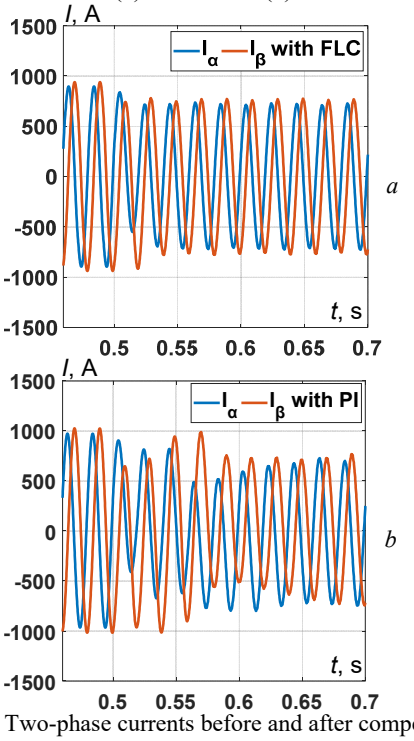

Fig. 19. Two-phase currents before and after compensation with FLC (*a*) and with PI (*b*) for Case II

Figures 18, 19 illustrate the three-phase and two-phase current waveform under HB-RPC-based FLC and PI control in response to variations in traction load. The three-phase side currents maintain stability amid changes in traction load.

Figure 20 shows the compensatory currents of the converter in FLC/HB-RPC and PI/HB-RPC, respectively. Following $t = 0.5$ s, the HB-RPC is activated. As depicted in Fig. 20, all power quality indices show enhancement and comply with the specifications outlined in the IEEE 1159 Standard. Therefore, drawing from the findings of the two cases, the suggested system has effectively mitigated grid-side nonlinear signal component, and current THDs.

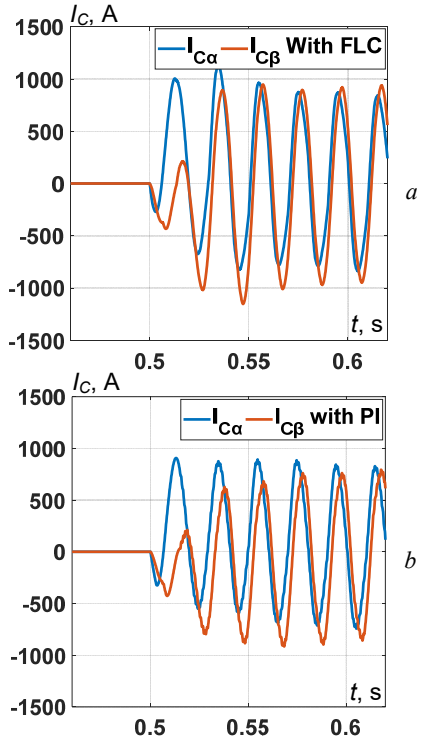

Fig. 20. Compensation current with FLC (*a*) and with PI (*b*) for Case II

NSC values for the FLC/HB-RPC are significantly lower compared to those of the PI/HB-RPC as illustrated in Fig. 21 and Table 5.

Table 6 displays the results of FFT analysis conducted both before and after current compensation for phases *A*, *B*, *C*. The data indicates that the HB-PRC and Ynev transformer, in conjunction with the FLC, outperform the PI controller in terms of harmonic elimination.

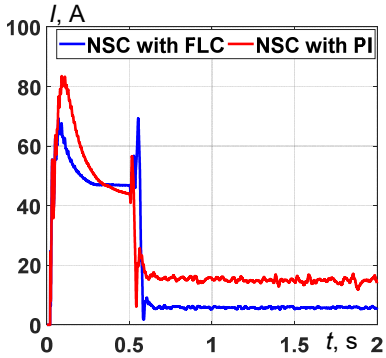

Fig. 21. Negative sequence currents with FLC and PI for Case II

Table 5

NSC ratio in the public electrical grid current with PI and FLC

HB-RPC integrate	Before	After
Time, s	0 – 0.4	0.5 – 2
PI, %	47.4	2.1
FLC, %		1.2

Table 6
THD compensation results

Cases 4 trains	I_A	I_B	I_C
Without compensation, %	25.37	16.05	39.55
Compensation / FLC, %	2.21	1.12	2.81
Compensation / PI, %	5.42	1.88	3.89

Conclusions. Addressing power quality issues in the traction power supply system of a high-speed railway equipped with Ynev wiring transformer. Ynev transformer is characterized by the capability to provide symmetrical two-phase current for traction loads and balanced three-phase current in railway system.

This study introduces a novel power quality control approach centered around half-bridge reactive power railway power conditioner (HB-RPC). The paper initially examines the mathematical model and control strategy of HB-RPC to improve the power quality in high-speed railway system. The use of adaptive fuzzy logic control is demonstrated to offer enhanced stability compared to PI control.

Through an analysis of two traction load scenarios, it is determined that HB-RPC, under adaptive fuzzy logic control, exhibits superior stability. Beyond improved stability, the response times are faster when compared to PI control, both during HB-RPC activation and changes in traction load. The use of fuzzy logic control ensures a combination of swift response and stability, thereby guaranteeing the reliable and efficient operation of HB-RPC. Both scenarios demonstrate that proposed system has superior stability and dynamic performance.

Conflict of interest. The authors declare that they have no conflicts of interest.

REFERENCES

1. Bharule S., Kidokoro T., Seta F. Evolution of High-Speed Rail and its Development Effects: Stylized Facts and Review of Relationships. *ADBI Working Paper Series*, 2019, no. 1040, 28 p. doi: https://doi.org/10.2139/ssrn.3554834.

2. Brenna M., Kaleybar H.J., Foiadelli F., Zaninelli D. Modern Power Quality Improvement Devices Applied to Electric Railway Systems. *2022 20th International Conference on Harmonics & Quality of Power (ICHQP)*, 2022, pp. 1-6. doi: https://doi.org/10.1109/ICHQP53011.2022.9808635.

3. Zare M., Varjani A.Y., Mohammad Dehghan S., Kavehei S. Power Quality Compensation and Power Flow Control in AC Railway Traction Power Systems. *2019 10th International Power Electronics, Drive Systems and Technologies Conference (PEDSTC)*, 2019, pp. 426-432. doi: https://doi.org/10.1109/PEDSTC.2019.8697653.

4. Wu S., Wu M., Wang Y. A Novel Co-Phase Power-Supply System Based on Modular Multilevel Converter for High-Speed Railway AT Traction Power-Supply System. *Energies*, 2021, vol. 14, no. 1, art. no. 253. doi: https://doi.org/10.3390/en14010253.

5. Barros L., Tanta M., Martins A., Afonso J., Pinto J. Evaluation of Static Synchronous Compensator and Rail Power Conditioner in Electrified Railway Systems Using V/V and Scott Power Transformers. *EAI Endorsed Transactions on Energy Web*, 2021, vol. 8, no. 34, art. no. 169164. doi: https://doi.org/10.4108/eai.29-3-2021.169164.

6. Tanta M., Pinto J.G., Monteiro V., Martins A.P., Carvalho A.S., Afonso J.L. Topologies and Operation Modes of Rail Power Conditioners in AC Traction Grids: Review and Comprehensive Comparison. *Energies*, 2020, vol. 13, no. 9, art. no. 2151. doi: https://doi.org/10.3390/en13092151.

7. Kryukov A., Cherepanov A., Avdienko I. Simulation of traction electricity supply systems equipped with unbalance-to-balance transformers. *AIP Conference Proceedings*, 2023, vol. 2700, no. 1, art. no. 040009. doi: https://doi.org/10.1063/5.0124856.

8. Boonlert T., Hongesombut K. Comparison of Voltage Distortion Impacts from High-Speed Railway Systems Connected to Electrical Grid Under Different Special Transformers. *2018 International Electrical Engineering Congress (IEECON)*, 2018, pp. 1-4. doi: https://doi.org/10.1109/IEECON.2018.8712124.

9. Roudsari H.M., Jalilian A., Jamali S. Half-Bridge Power Quality Conditioner for Railway Traction Distribution System Based on a New Balancing Transformer. *2018 Electrical Power Distribution Conference (EPDC)*, 2018, pp. 1-7. doi: https://doi.org/10.1109/EPDC.2018.8536270.

10. Reddy C.V.K., Das G.T.R., Krishna Veni K. Analysis of AC Transmission System Using Fuzzy Logic Controller for Damping of Low Frequency Oscillations with Interline Power Flow Controller. *International Journal of Applied Engineering Research*, 2019, vol. 14, no 9, pp. 2148-2155.

11. Lao K.W., Wong M.C., Santoso S. Recent Advances of FACTS Devices for Power Quality Compensation in Railway Traction Power Supply. *2018 IEEE/PES Transmission and Distribution Conference and Exposition (T&D)*, 2018, pp. 1-5. doi: https://doi.org/10.1109/TDC.2018.8440270.

12. Afonso J.L., Tanta M., Pinto J.G.O., Monteiro L.F.C., Machado L., Sousa T.J.C., Monteiro V. A Review on Power Electronics Technologies for Power Quality Improvement. *Energies*, 2021, vol. 14, no. 24, art. no. 8585. doi: https://doi.org/10.3390/en14248585.

13. Mohamed S.A. Enhancement of power quality for load compensation using three different FACTS devices based on optimized technique. *International Transactions on Electrical Energy Systems*, 2020, vol. 30, no. 3. art. no. e12196. doi: https://doi.org/10.1002/2050-7038.12196.

14. Tasiu I.A., Liu Z., Wu S., Yu W., Al-Barashi M., Ojo J.O. Review of Recent Control Strategies for the Traction Converters in High-Speed Train. *IEEE Transactions on Transportation Electrification*, 2022, vol. 8, no. 2, pp. 2311-2333. doi: https://doi.org/10.1109/TTE.2022.3140470.

15. Sujatha M.S., Sreelakshmi S., Parimalasundar E., Suresh K. Mitigation of harmonics for five level multilevel inverter with fuzzy logic controller. *Electrical Engineering & Electromechanics*, 2023, no. 4, pp. 52-56. doi: https://doi.org/10.20998/2074-272X.2023.4.08.

16. Chaib Ras A., Bouzerara R., Bouzeria H., Aissaoui M., Mammeri I. An Efficient Strategy for Power Quality Conditioner with Half-Bridge for High-Speed Railway. *Lecture Notes in Networks and Systems*, 2021, vol. 174, pp. 894-901. doi: https://doi.org/10.1007/978-3-030-63846-7_87.

17. Cui G., Luo L., Liang C., Hu S., Li Y., Cao Y., Xie B., Xu J., Zhang Z., Liu Y., Wang T. Supercapacitor Integrated Railway Static Power Conditioner for Regenerative Braking Energy Recycling and Power Quality Improvement of High-Speed Railway System. *IEEE Transactions on Transportation Electrification*, 2019, vol. 5, no. 3, pp. 702-714. doi: https://doi.org/10.1109/TTE.2019.2936686.

18. Zhao S., Huang X., Fang Y., Zhang H. DC-Link-Fluctuation-Resistant Predictive Torque Control for Railway Traction Permanent Magnet Synchronous Motor in the Six-Step Operation. *IEEE Transactions on Power Electronics*, 2020, vol. 35, no. 10, pp. 10982-10993. doi: https://doi.org/10.1109/TPEL.2020.2975497.

19. Dai X. Negative Sequence Compensation Method for High-Speed Railway With Integrated Photovoltaic Generation System. *CPSS Transactions on Power Electronics and Applications*, 2022, vol. 7, no. 2, pp. 130-138. doi: https://doi.org/10.24295/CPSSTPEA.2022.00012.

20. Ikhe A., Pahariya Y. Voltage regulation using three phase electric spring by fuzzy logic controller. *Electrical Engineering & Electromechanics*, 2023, no. 4, pp. 14-18. doi: https://doi.org/10.20998/2074-272X.2023.4.02.

21. Gopal Reddy S., Ganapathy S., Manikandan M. Power quality improvement in distribution system based on dynamic voltage restorer using PI tuned fuzzy logic controller. *Electrical Engineering & Electromechanics*, 2022, no. 1, pp. 44-50. doi: https://doi.org/10.20998/2074-272X.2022.1.06.

Received 11.08.2023
Accepted 13.11.2023
Published 02.03.2024

A. Chaib Ras[1], *PhD,*
R. Bouzerara[1], *Professor,*
H. Bouzeria[1], *Doctor, Associate Professor,*
[1] Transportation Engineering Department,
University of Constantine 1,
Route d'Ain ElBey, 25000, Constantine, Algeria,
e-mail: amira.chaibras@student.umc.edu.dz (Corresponding Author);
bouzerara.ramdane@umc.edu.dz; bouzeria.hamza@umc.edu.dz

How to cite this article:
Chaib Ras A., Bouzerara R., Bouzeria H. An adaptive controller for power quality control in high speed railway with electric locomotives with asynchronous traction motors. *Electrical Engineering & Electromechanics*, 2024, no. 2, pp. 23-30. doi: https://doi.org/10.20998/2074-272X.2024.2.04